

Tight-binding study of structure and vibrations of amorphous silicon

J. L. Feldman, N. Bernstein, D. A. Papaconstantopoulos, and M. J. Mehl

Center for Computational Materials Science, Naval Research Laboratory, Washington, DC 20375

(dated: November 30, 2021)

We present a tight-binding calculation that, for the first time, accurately describes the structural, vibrational and elastic properties of amorphous silicon. We compute the interatomic force constants and find an unphysical feature of the Stillinger-Weber empirical potential that correlates with a much noted error in the radial distribution function associated with that potential. We also find that the intrinsic first peak of the radial distribution function is asymmetric, contrary to usual assumptions made in the analysis of diffraction data. We use our results for the normal mode frequencies and polarization vectors to obtain the zero-point broadening effect on the radial distribution function, enabling us to directly compare theory and a high resolution x-ray diffraction experiment.

PACS numbers: 61.43.Dg, 62.20.Dc, 63.50.+x, 78.55.Qr

Amorphous silicon (a-Si) is a prototype for continuous-random-network covalent glasses that, with some hydrogen content, has technological applications as a relatively inexpensive electronic material. While the basic structure of a-Si is believed to be a four-fold-coordinated continuous random network, detailed information about network connectivity and defects is lacking. Atomic resolution structure is very difficult to determine directly, and experiments have relied on unusual or indirect probes such as variance coherence microscopy [1] and Raman spectroscopy [2, 3] as well as on more standard techniques such as diffraction [4, 5] and EXAFS [6, 7]. The experimental measurements suggest significant deviation from a continuous random network, including average coordination that is significantly less than 4 (e.g. Ref. 5) and that unannealed samples may be paracrystalline [1]. Many empirical-potential simulations have been done, but it is not clear if empirical potentials are accurate enough to give reliable results for properties, such as coordination defects, that depend on bond breaking and bond formation. A number of simulations of a-Si structure have used electronic-structure based methods, which are generally among the most reliable for solid state systems (e.g. Refs. 8, 9, 10, 11). However, none have carefully compared the radial distribution function (RDF) to high resolution experiments [5], and none included quantum-mechanical vibrational effects. Another important question concerns the vibrational properties of a-Si, which give us information about the structure and the interactions of atoms in the material. The vibrational density of states (VDOS) was measured experimentally using inelastic neutron scattering (INS) [32]. Empirical-potential simulations have been used to analyze vibrational properties in detail [12], but all show significant errors in the shape of the VDOS or in other properties. While the VDOS of a-Si has been simulated with electronic structure methods [8, 13, 14], the underlying force constants themselves have not been analyzed. There have been many studies of force constants in crystalline Si, which shows unusual phonon dispersion and force con-

stants that oscillate in magnitude as a function of distance [15, 16].

We study the elastic constants, vibrational properties, and structure of a-Si using a tight-binding (TB) total-energy method. We find elastic constants and VDOS that are in good agreement with experiment, and qualitatively better than empirical-potential simulations. The structure has a sharp first-neighbor RDF peak that agrees very well with experiment when zero-point and thermal broadening is included. This peak is significantly non-Gaussian, calling into question the coordination-statistics analysis of previous diffraction experiments.

We use the Naval Research Laboratory (NRL) TB method [17, 18]. The non-orthogonal sp^3 -basis TB model has been shown to accurately describe the elastic constants and phonon dispersion in crystalline Si and the electronic density of states for a highly defected amorphous model [18]. To generate the a-Si models we relax using TB-calculated forces a-Si models generated by other techniques. The NRL-TB model is used to calculate the energy of the structure and the atomic forces [21]. The conjugate-gradient method is applied to find mechanical-equilibrium positions at a fixed volume, employing the criterion that components of atomic forces be less than 10^{-3} eV/Å. The relaxation procedure is carried out at several volumes to obtain results at zero pressure, but components of the stress tensor, generally of magnitude less than 0.8 GPa, remain.

One model, which we denote TB1, is generated by relaxing (using TB) a 216 atom perfect continuous-random-network model [19] with periodic boundary conditions relaxed with a Keating interatomic potential [20]. The TB-relaxed model is perfectly four-fold coordinated, with 1.3% lower density than the crystal, compared to 1.7% lower density measured experimentally [5]. The bond-angle distribution has a RMS deviation of 11 from the average value of 109.2° , in close agreement with relaxed *ab initio* calculation [10] and analysis of experiment [4]. A second model, which we denote TB2, is generated by relaxing a structure from a molecular-dynamics simulation

TABLE I: Selected elastic constants c , bulk modulus B and Young's modulus E (10^{11} dyn/cm²). The index i varies from 1 to 3, and j from 4 to 6.

	TB1	TB2	Exp./FP	SW ^(a)
c_{ii}	16.31-16.45	15.06-16.00	13.8 ^(b) , 17 (2) ^(c)	11.94-13.11
c_{jj}	5.68-5.84	5.26-5.56	4.8 ^(b) , 4.5 ^(a)	2.54-3.21
$c_p^{(d)}$	5.77	5.06	"	2.62
c_{12}	4.77	5.32		6.69
B	8.73	8.99	5.9 ^(e) , 8.25 ^(f)	8.52
E	14 ^(g)	13 ^(g)	12.4 (3) ^(a)	7 ^(g)
	11.7 (5)-13.4 (5) ^(h)			

(a) Ref. 24; (b) Ref. 25; (c) Ref. 26;

(d) Defined here as $(c_{11}-c_{12})/2$; (e) Ref. 27

(f) Ref. 10; (g) based on values of c_{12} and c_p ;

(h) Ref. 28.

of the rapid quenching of liquid Si using the environment dependent interatomic potential [22]. The TB2 structure is slightly more dense than TB1, but still about 0.5% less dense than the crystal. The energy is 28 meV/atom lower than the TB1 energy, despite the presence of 6% 5-fold and 0.46% 3-fold coordinated atoms (corresponding to an average coordination of 4.05) [23]. The RMS bond-angle deviation is 12.5°, although the distribution has wide, non-Gaussian wings; excluding 2% of the bond-angles reduces the RMS deviation to 10.4°. We also show some comparisons with results using the Stillinger-Weber (SW) interatomic potential [29]. The SW potential, which includes radial and bond-angle terms, is one of the most often used potentials for simulations of Si. We use a structure (Ref. 24, Table II, model IV) generated by relaxing with SW the same starting structure as TB1. Finally, we note that while it is possible to use electronic structure methods to generate amorphous structures from procedures that are less dependent on the initial structure, it is very expensive computationally. The difficulty in fully annealing the structure seems to lead to a consistent overestimate of the width of the first-neighbor peak in the RDF [8, 9].

The relaxed static lattice TB elastic constants c_{ij} were obtained by the method of homogeneous deformation. The TB results [31] are compared in Table I with results of first-principles (FP) [10] calculations, SW calculations, and several experiments on dense samples (a wider range of shear values are quoted in Table V of Ref. 30). Although there is some deviation between the two TB structures it is small. While ultrasonic measurements of elastic properties are not available for a-Si, the Young's modulus E can be measured with a vibrating reed apparatus, and other elastic constants can be inferred from spectroscopic studies. Our TB results for both models are close to the experimental values, although our value of c_{44} is likely 10-20% too large. The SW empirical potential results are significantly worse in comparison with experiment.

The VDOS is calculated from a dynamical ma-

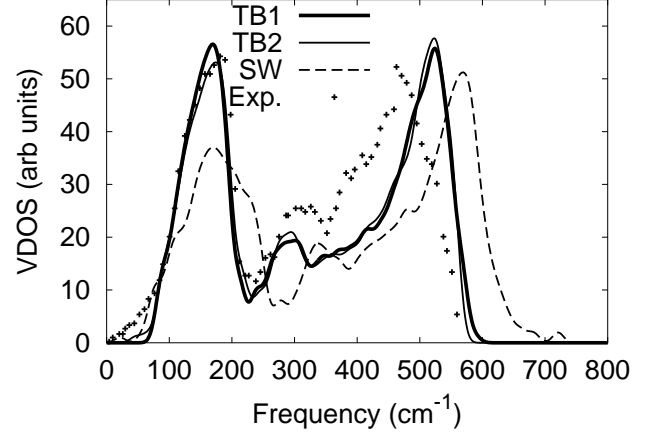


FIG. 1: Vibrational density of states of a-Si. A Gaussian broadening of FWHM = 20 cm⁻¹ is employed. The experimental data are from Ref. [32].

trix approach. The matrix elements $\langle i; j \rangle$

$F_{ij}(i) = u_{ij}(j)$ are calculated using the TB forces with a central-finite difference approach that eliminates all odd-order anharmonic terms in the potential energy [33]. The TB VDOS for structures TB1 and TB2 are compared with SW results and INS [32] measurements in Fig. 1. For both structures the TB calculation yields the overall shape very well; it exactly describes the low frequency TA peak, gives a slightly too small frequency of the LA peak (300 cm⁻¹) and about a 10% percent too high frequency of the high frequency TO peak. The TB results are a qualitative improvement over results based on the SW potential, as shown in the figure, and they are in good agreement with ab initio results for a 216 atom structural model [14].

The range of the effective interactions in the solid can give us information about the physics of the interactions, and can guide the development of approximations such as empirical potentials. In Fig. 2 we plot all of the cartesian force constants between pairs of atoms with interatomic distances less than 10 Å. The difference in range between the SW results and the TB results is easy to see: The SW interactions are large up to about 3.5 Å, and go to exactly zero at twice the SW cutoff of 3.75 Å. The TB interactions are already quite small at 2.8 Å, but do not go to zero even at 10 Å. This comparison of TB and SW leads to a view of interactions in the solid that is more subtle than the usual assumption that empirical potentials are short ranged and that the real interactions are long ranged: The SW potential interactions go to zero at a range that is too short, but at intermediate distances the interactions are too strong. We also note that the preponderance of force constants as a function of interatomic distance give a clear envelope function that has an oscillatory behavior which matches the RDF peak positions. This is qualitatively similar to the case of the crystal,

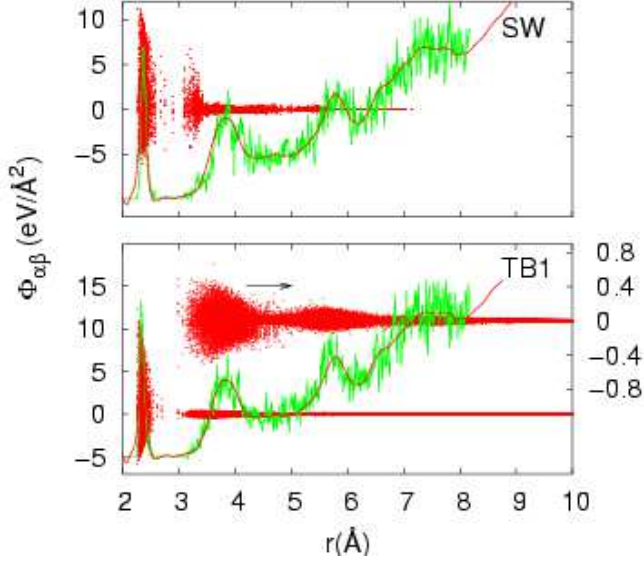


FIG. 2: Force constants between pairs of atoms in SW (top) and TB1 (bottom) relaxed structures (dots). Superimposed are the corresponding $J(r)$ functions (jagged lines) in arbitrary units and the experimental, annealed-sample, results of Ref. [5] for $J(r)$ (smooth lines). The upper scatterplot in the TB panel is a magnification of the smaller magnitude force constants.

even though the explanations for the oscillation in the crystal do not apply to the amorphous structure [15, 16].

The problem with the SW potential is a direct consequence of the form of the potential. In the amorphous there are pairs of atoms in the second-neighbor peak with distances smaller than the SW cutoff. It is clear from the TB force constants that the effective interactions for these pairs is qualitatively different from the first-neighbor interactions. However, in the SW simulation these second-neighbor pairs interact through terms that are meant to describe the interactions of first-neighbor atoms. In particular, the two-body contribution has strong negative curvature at these distances, and the three-body terms include contributions from triplets with a vertex angle that does not correspond to an atom with two sp^3 orbitals in bonding configurations. These two types of contributions lead to the unphysically large force constants in the SW results at this range of distances. The range of incorrect force constants also coincides with the shoulder in the SW RDF that is not observed in our TB results or in the experimental measurements [34].

The distribution of force constants gives us information about the types of effective interactions between bonded atoms. Under the first peak of the RDF the largest positive cartesian force constants are twice the magnitude of the largest negative force constants for both SW and TB. This relation is consistent with an effective bond-stretching interaction for first-neighbors. We plot the results for the bond-stretching components in a plot as

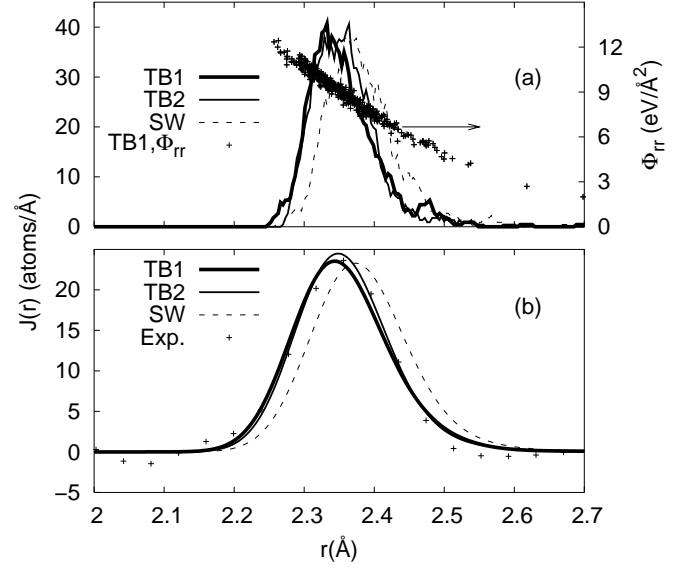


FIG. 3: (a) First peak of the static RDF and TB1 bond stretching force constants. (b) Broadened results corresponding to $T = 10K$ in comparison with experiment (annealed sample) [5].

a function of r (Fig. 3a). The radial force constants decrease with increasing r as one expects from a physically reasonable first-neighbor bonding potential. Pairs with large (small) interatomic bond stretching force constants will have small (large) relative mean square displacements, so these results clearly have an impact on the nature of the broadening of the RDF.

Very little attention has been given in the literature to the shape of the first peak in the RDF $J(r)$ [5]. This peak has been measured very carefully at $T = 10 K$ with x-ray diffraction, using high energy photons and high resolution, i.e., large Q_{max} , by Laaziri et al. [5]. They obtain a fit of their data to a Gaussian, with average coordination of 3.88 ± 0.1 (3.79 ± 0.1) for the annealed (unannealed) sample. In Fig. 3a we plot the first peak of the static $J(r)$ for models TB1 and TB2, and the SW results. The TB static peak is asymmetric, and its width is significantly larger than the static-disorder estimate by Laaziri et al. In order to compare directly with the experimental $J(r)$ it is necessary to properly take account of the zero-point and thermal broadening. The quantity measured by the x-ray experiment is, in the small displacement limit,

$$J(r) = \frac{1}{N} \sum_{i,j=1}^N \frac{1}{2 U_{ij}^r} \exp(-(\hat{r}_{ij} - r)^2 / (2 U_{ij}^r));$$

where $U_{ij}^r = \langle (\hat{r}_{ij} - \bar{r}_{ij})^2 \rangle$. Thus we need the mean-squared relative displacements, for pairs of atoms, along the interatomic vector direction. We calculate them within the harmonic approximation at $T = 10 K$ using

our computed vibrational modes. Since $T = 10$ K essentially corresponds to $T = 0$ K for these considerations, what we obtain is the minimum measurable width for the first peak in the RDF of amorphous silicon. As seen in Fig. 3b the results are in agreement with experiment, aside from a small skewing of the theoretical function to large r . Although it has not been observed in a-Si, this type of asymmetry has been observed in EXAFS of amorphous germanium [36]. Both the TB1 and TB2 models, despite the very different originating structure and differences in coordination defects, show nearly identical RDF

first peaks. The good agreement with experiment of the broadened RDF suggests that our static peak width is correct, and that Laaziri et al. underestimate the static disorder contribution to the broadening. This may be caused by inaccuracy in the polycrystalline $J(r)$ that is used to estimate the dynamic broadening. In the experiment a lower Q_{max} (35 \AA^{-1}) was used for the polycrystal than for the amorphous structure (55 \AA^{-1}), although the former is expected to have a narrower first peak. Numerous other treatments using EXAFS or diffraction have not been considered here because they all use too low values of Q_{max} for obtaining reliable information on the first peak. The only other theoretical study of quantum effects in $J(r)$ is by Herrero [5], who used the SW potential but treated the quantum effects on the nuclear vibrations exactly. Our results using the SW potential are presented in Fig. 3. The result for the amount of zero-point broadening is consistent with Herrero's work, although due to differing approximations a direct comparison is not possible. We note that the Wooten model on which both the SW and TB1 models are based yields a static $J(r)$ (not shown) that is quite symmetric, and as broad as the experimental breadth.

To conclude, we have shown that the NRL-TB method can reliably compute structural, vibrational, and elastic properties of a-Si. The results are nearly identical for two structural models, one with perfect four-fold coordination and one with several atomic percent coordination defects. We have presented the first discussion of force constants in a-Si, which has revealed limitations of the most frequently used empirical potential for silicon. Our calculated elastic constants fall within the range of experimental values for imperfect samples prepared under various conditions. We have also carefully studied the first peak in the radial distribution function. We observe a clear asymmetric peak in the case of the static quantity which is not observable experimentally. We have included the (essentially) zero-point broadening effects in $J(r)$ to obtain the experimentally measured quantity. Our two structural models, which have average coordinations of 4.00 and 4.05, respectively, reproduce the first peak in the experimental $J(r)$ (for the annealed sample) except for a slight asymmetry still present in the broadened result. We believe that such an asymmetry is expected on physical grounds and that perhaps it has

been "missed" experimentally because of the challenging analysis required to obtain $J(r)$ from the diffraction results.

This work was supported by the U.S. Office of Naval Research. We are also grateful to Dr. S. Roorda for a helpful communication and for sending us the x-ray data of Ref. [5] for the radial distribution function. We thank Dr. S. Richardson for a helpful conversation.

-
- [1] M. M. J. Treacy, J. M. Gibson, and P. J. Keblinski, *J. of Non-Cryst. Solids*, **231**, 99 (1998).
 - [2] D. Beeman, R. Tsu, and M. F. Thorpe, *Phys. Rev. B* **32**, 874 (1985).
 - [3] R. L. C. Vink, G. T. Barkema, and W. F. van der Weg, *Phys. Rev. B* **63**, 115210 (2001) and references therein.
 - [4] J. Fortner and J. S. Lannin, *Phys. Rev. B* **39**, 5527 (1989).
 - [5] K. Laaziri, S. Kycia, S. Roorda, M. Chicoine, J. L. Robertson, J. Wang, and S. C. Moss, *Phys. Rev. Lett.*, **82**, 3460 (1999) and references therein; *ibid.*, *Phys. Rev. B* **60**, 13520 (1999).
 - [6] M. Wakagi, K. Ogata, and A. Nakano, *Phys. Rev. B* **50**, 10666 (1994-I); A. Filipponi, F. Evangelisti, M. Benfatto, S. Mobilio, and C. R. Natoli, *Phys. Rev. B* **40**, 9636 (1989).
 - [7] C. J. Glover, G. J. Foran, and M. C. Ridgway, *Nuc. Instr. and Methods in Physics Res. B* **199**, 195 (2003).
 - [8] E. G. I. Stich, R. Car, and M. Parrinello, *Phys. Rev. B* **44**, 11092 (1991-II).
 - [9] P. Biswas, *Phys. Lett. A* **282**, 294 (2001).
 - [10] M. Durandurdu and D. A. Dabold, *Phys. Rev. B* **64**, 014101 (2001).
 - [11] P. Klein, H. M. Urbassek, and T. Frauenheim, *Comp. Mat. Sci.* **13**, 252 (1999).
 - [12] P. B. Allen, J. L. Feldman, J. Fabian, and F. Wooten, *Phil. Mag. B* **79**, 1715 (1999).
 - [13] P. Biswas, *Phys. Rev. B* **65**, 125208 (2002).
 - [14] S. M. Nakhmanson and D. A. Dabold, *J. of Non-Cryst. Solids*, **266-269**, 156 (2000).
 - [15] E. O. Kane, *Phys. Rev. B* **31**, 7865 (1985).
 - [16] G. M. Rignanese, J.-P. Michenaud, and X. Gonze, *Phys. Rev. B* **53**, 4488 (1996).
 - [17] R. E. Cohen, M. J. Mehl, and D. A. Papaconstantopoulos, *Phys. Rev. B* **50**, 14695 (1994); M. J. Mehl and D. A. Papaconstantopoulos, *ibid.*, **54**, 4519 (1996).
 - [18] N. Bernstein, M. J. Mehl, D. A. Papaconstantopoulos, N. I. Papanicolaou, M. Z. Bazant, and E. Kaxiras, *Phys. Rev. B* **62**, 4477 (2000); *ibid.*, **65**, 249902 (2002) (E).
 - [19] F. Wooten, private communication.
 - [20] F. Wooten, K. Winer, and D. Weaire, *Phys. Rev. Lett.* **54**, 1392 (1985).
 - [21] F. Kirchhoff, M. J. Mehl, N. I. Papanicolaou, D. A. Papaconstantopoulos, and F. S. Khan, *Phys. Rev. B* **63**, 195101 (2001).
 - [22] M. Bazant, private communication; see also J. F. Justo, M. Z. Bazant, E. Kaxiras, V. V. Bulatov, and S. Yip, *Phys. Rev. B* **58**, 2539 (1998).
 - [23] Although this energy difference suggests the possibility of energetically favorable coordination defects, the small system sizes and minimal annealing make this conclusion

uncertain.

- [24] J.L. Feldman, J.Q. Broughton, and F. Wooten, Phys. Rev. B 43, 2152 (1991) and references therein.
- [25] X. Zhang, J.D. Comins, A.G. Every, P.R. Stoddart, W. Pang, and T.E. Derry, Phys. Rev. B 58, 13677 (1998).
- [26] M. Grimsditch, W. Senn, G. Winterling, and M.H. Brodsky, Sol. State Comm. 26, 229 (1978).
- [27] K. Tanaka, Sol. State Comm. 60, 295 (1986).
- [28] Kuschnereit et al., Applied Phys. A (Mat. Sci. and Proc.) 61, 269 (1995).
- [29] F.H. Stillinger and T.A. Weber, Phys. Rev. B 31, 5262 (1985).
- [30] R.O. Pohl, X. Liu, and E. Thompson, Rev. of Mod. Phys. 74, 991 (2002).
- [31] Due to finite-size effects, our results do not exactly satisfy the expected isotropy conditions on the elastic constants of an amorphous material.
- [32] W.A. Kamitakahara, C.M. Soukoulis, H.R. Shanks, U. Buchenau, and G.S. Grest, Phys. Rev. B 36, 6539 (1987).
- [33] We tacitly assume that the cell size is big enough that the force on an atom due to the displacement of a different atom and that of its periodic images can be ascribed solely to the closest displaced atom.
- [34] R.L.C. Vink, G.T. Barkema, W.F. van der Weg, and N. Mousseau, J. Non-Cryst. Solids, 282, 248 (2001).
- [35] C.P. Herrero, Europhys. Lett. 44, 734 (1998); C.P. Herrero, J. of Non-Cryst. Solids 271, 18 (2000).
- [36] M.C. Ridgway, C.J. Glover, K.M. Yu, G.J. Foran, C. Clerc, J.L. Hansen, and A.N. Larsen, Phys. Rev. B 61, 12586 (2000).